Living Radical Polymerization of Bipolar Transport Materials for Highly Efficient Light Emitting Diodes

Lan Deng,[†] Paul T. Furuta,[†] Simona Garon,[‡] Jian Li,[‡] David Kavulak,[†] Mark E. Thompson,[‡] and Jean M. J. Fréchet*,[†]

Material Sciences Division, Lawrence Berkeley National Laboratory, and Department of Chemistry, University of California, Berkeley, California 94720-1460, and Department of Chemistry, University of Southern California, Los Angeles, California 90089-0744

Received August 25, 2005. Revised Manuscript Received November 13, 2005

The synthesis of hole transport, electron transport, and functionalized β-diketone monomers, as well as their living radical polymerization, is described. Utilizing a second-generation nitroxide initiator allows the polymerization of homopolymers, as well as random and block co- and terpolymers, with predictable molecular weights and low polydispersities. These highly soluble polymers bearing bipolar transport moieties can either be used directly as a matrix for doping with luminescent molecules or be functionalized with phosphorescent iridium or platinum complexes. The flexibility of polymer construction and functionalization translates into versatility in the design and the tuning of functional properties of solution-processed organic light emitting diodes. Devices emitting white light with maximum front face external quantum efficiency (EQE) of 4.9% and devices having green emission with maximum EQE of 10.5% have been achieved.

Introduction

Electroactive materials have attracted much attention because of their use in emerging technologies[1] such as organic light emitting diodes (OLEDs),[2] photovoltaic devices,[3] and field effect transistors.[4] In OLEDs, high quantum efficiencies were obtained when small, molecular phosphorescent emitters such as cyclometalated platinum[5] and iridium[6] complexes were used. The strong spin−orbital coupling of heavy metals facilitates efficient intersystem crossing and allows the complexes to capture both the electrogenerated singlet and the electrogenerated triplet excitons. Thus, devices based on these complexes can theoretically approach 100% internal quantum efficiency.

While the best performances have typically been obtained with devices based on small molecules, polymers[7] and dendrimers[8] are of great interest as they are more amenable to the solution processing techniques such as spin-coating and ink-jet printing that could be used for low cost production over large areas. A particularly appealing solution to achieve highly efficient polymer-based devices involves energy or charge transfer from polymer hosts to phosphorescent guest molecules. Both conjugated and nonconjugated linear polymer hosts utilizing phosphorescent complexes as dopants[7a−d] or incorporating them in the side chains[7e,f] have been reported. However, the use of conjugated polymers as hosts can be problematic because they can quench triplet excitons from phosphors emitting wavelengths lower than red.[9] Therefore, polymers with a nonconjugated backbone may be more suitable for use with phosphorescent emitters. In addition, nonconjugated polymers generally have greater solubility than rigid-rod conjugated polymers, thus facilitating their application to solution-processed devices.

In devices with a single emitting layer, the balance of holes and electrons is very important for efficient performance. Several reports[10] have shown that doping oxadiazole electron transport (ET) molecules into a polymeric hole transport (HT)

* To whom correspondence should be addressed. E-mail: frechet@berkeley.edu.
† University of California.
‡ University of Southern California.

(1) Yu, G.; Heeger, A. J. *Synth. Met.* **1997**, *85*, 1183.
(2) (a) Burroughes, J. H.; Bradley, D. D. C.; Brown, A. R.; Marks, R. N.; Mackay, K.; Friend, R. H.; Burns, P. L.; Holmes, A. B. *Nature* **1990**, *347*, 539. (b) Kido, J.; Nagai, K.; Okamoto, Y.; Stotheim, T. *Appl. Phys. Lett.* **1991**, *59*, 2760.
(3) (a) Frank, A. J.; Glenis, S.; Nelson, A. J. *J. Phys. Chem.* **1989**, *93*, 3818. (b) Antoniadis, H.; Hsieh, B. R.; Abkowitz, M. A.; Jenekhe, S. A.; Stolka, M. *Synth. Met.* **1994**, *62*, 265. (c) Yu, G.; Heeger, A. J. *J. Appl. Phys.* **1995**, *78*, 4510.
(4) (a) Garnier, F. *Chem. Phys.* **1998**, *227*, 253. (b) Koezuka, H.; Tsumura, A. *Synth. Met.* **1989**, *28*, 753. (c) Murphy, A. R.; Fréchet, J. M. J.; Chang, P.; Lee, J.; Subramanian, V. *J. Am. Chem. Soc.* **2004**, *126*, 1596. (d) Murphy, A. R.; Liu, J.; Luscombe, C.; Kavulak, D.; Fréchet, J. M. J.; Kline, R. J.; McGehee, M. D. *Chem. Mater.* **2005**, *17*, 4892.
(5) (a) O'Brien, D. F.; Baldo, M. A.; Thompson, M. E.; Forrest, S. R. *Appl. Phys. Lett.* **1999**, *74*, 442. (b) Chan, S.-C.; Chan, M. C. W.; Wang, Y.; Che, C.-M.; Cheung, K.-K.; Zhu, N. *Chem.—Eur. J.* **2001**, *7*, 4180. (c) Lu, W.; Mi, B.-X.; Chan, M. C. W.; Hui, Z.; Che, C.-M.; Zhu, N.; Lee, S.-T. *J. Am. Chem. Soc.* **2004**, *126*, 4958.
(6) (a) Baldo, M. A.; Lamansky, S.; Burrows, P. E.; Thompson, M. E.; Forrest, S. R. *Appl. Phys. Lett.* **1999**, *75*, 4. (b) Adachi, C.; Baldo, M. A.; Forrest, S. R.; Thompson, M. E. *Appl. Phys. Lett.* **2000**, *77*, 904.
(7) (a) Lee, C.-L.; Lee, K. B.; Kim, J.-J. *Appl. Phys. Lett.* **2000**, *77*, 2280. (b) Jiang, X.; Register, R. A.; Killeen, K. A.; Thompson, M. E.; Pschenitzka, F.; Sturm, J. C. *Chem. Mater.* **2000**, *12*, 2542. (c) Vaeth, K. M.; Tang, C. W. *J. Appl. Phys.* **2002**, *92*, 3447. (d) Gong, X.; Moses, D.; Heeger, A. J.; Xiao, S. *J. Phys. Chem. B* **2004**, *108*, 8601. (e) Suzuki, M.; Tokito, S. Sato, F.; Igarashi, T.; Kondo, K.; Koyama, T.; Yamaguchi, T. *Appl. Phys. Lett.* **2005**, *86*, 103507. (f) Furuta, P. T.; Deng, L.; Garon, S.; Thompson, M. E.; Fréchet, J. M. J. *J. Am. Chem. Soc.* **2004**, *126*, 15388.
(8) (a) Markham, J. P. J.; Lo, S. C.; Magennis, S. W.; Burn, P. L.; Samuel, I. D. W. *Appl. Phys. Lett.* **2002**, *80*, 2645. (b) Furuta, P.; Brooks, J.; Thompson, M. E.; Frechet, J. M. J. *J. Am. Chem. Soc.* **2003**, *125*, 13165.
(9) (a) Sudhakar, M.; Djurovich, P. I.; Hogen-Esch, T. E.; Thompson, M. E. *J. Am. Chem. Soc.* **2003**, *125*, 7796. (b) Chen, X.; Liao, J. L.; Liang, Y.; Ahmed, M. O.; Tseng, H. E.; Chen, S. A. *J. Am. Chem. Soc.* **2003**, *125*, 636.

10.1021/cm051922+ CCC: $33.50
Published on Web 12/22/2005

material has beneficial effects on the performance of solution-processed devices. Bazan and co-workers have reported a high quantum efficiency of 10% for devices obtained by doping tris[9,9-dihexyl-2-(pyridinyl-2′)fluorene]iridium(III) into a blend of 2-*tert*-butylphenyl-5-biphenyl-1,3,4-oxadiazole (PBD) and poly(vinylcarbazole).[10a] Jiang et al. have also reported achieving a quantum efficiency of 12% by doping iridium(III) bis(2-phenylquinolyl)-N,C$^{2'}$) acetylacetonate into a blend of polyhedral oligomeric silsesquioxane-terminated poly(9,9-dioctylfluorene) and PBD.[10b] However, these efficiencies were obtained by measuring the total light output using an integrating sphere. The external quantum efficiency measured by this method could be up to four times larger than that measured in the viewing direction only (usually the front face), typically referred to as the EQE.[11,12]

Incorporating both HT and ET functionalities into copolymers has an additional advantage over the ET doping strategy involving small molecules in that the homogeneity of the covalently linked functionalities could prevent the gross phase separation and eventual crystallization of molecular ET. We have recently reported[7f] a random terpolymer with a pendant ET, HT, and platinum complex that emits white light with an EQE of 4.6%. More recently, Suzuki et al. have reported a terpolymer with a pendant iridium complex emitting green light with 11.8% EQE using Cs as the cathode.[7e] However, the influence of different ET and HT moieties, as well as the nature of the polymer backbone on device performance, has not been fully explored.

Living radical polymerization[13] has been shown to be a convenient method for preparing homopolymers, statistically random and block copolymers, and even graft and branched copolymers with low polydispersities, predictable molecular weights (MWs), and controlled architecture. Of the available living radical polymerization methods, nitroxide-mediated free radical polymerization (NMRP) is of particular interest for synthesizing electroactive polymers because of its tolerance of many functional groups,[14] as well as the absence of metal catalysts, coordinating ligands, or sulfur-containing moieties. This is in contrast to other excellent methods of living polymerization, such as atom transfer radical polymerization, ring opening metathesis polymerization, or reversible addition-fragmentation chain transfer polymerization. Such consideration is important for the intended end use of the materials, as ligand functionalized monomers will be incorporated in the polymers, and the presence of catalyst residues might impair device performance. Boiteau et al.[15] have reported a TEMPO (2,2,6,6-Tetramethyl-1-piperidinyloxy) initiated polymerization of a block copolymer composed of an oligo-phenylenevinylene block and an oxadiazole block. Though the polymers reported had modest polydispersities and conversions, this work demonstrated that NMRP was suitable for the controlled synthesis of electroactive block copolymers with a nonconjugated backbone. Behl et al.[16] have also presented TEMPO initiated HT/ET block copolymer synthesis, with good polydispersities reported for their solution-based polymerizations.

Compared to TEMPO, the use of newer generation alkoxyamine-based initiators[14] can produce materials with lower polydispersity, which is a very important factor in achieving well-defined morphology in block copolymers. When compared to random copolymers, block copolymers offer more tunability via morphological effects on substrate interfaces or the degree of component phase separation. Certain morphologies may also be able to directionally guide the light, maximizing the amount of light emitted from the front face of the device.[17] Self-assembly to patterned surfaces might even enable the construction of nanosized molecular electronics. We now report the synthesis of HT, ET, and β-diketone ligand (Ln) monomers, as well as their polymerization using an alkoxyamine initiator—a modular approach to the generation of both random and block copolymers with bipolar transport abilities. We demonstrate that these materials, whether simply used as a matrix for doping with phosphorescent emitters or functionalized with platinum or iridium phosphor complexes, can be used to construct highly efficient, solution-processed OLEDs.

Results and Discussion

Monomers. A series of both styrenic and acrylic HT and ET monomers were constructed in order to evaluate their suitability for the synthesis of electroactive materials. In Scheme 1, 3-vinyl triphenylamines **2** and **3** were constructed from the corresponding diphenylamines and 3-bromostyrene utilizing NaO-*t*-Bu as the base. Amination of **1** with carbazole proceeded similarly when a stronger base, NaH, was used at 80 °C, giving monomer **4**. Acrylate **6** was constructed from alcohol **5**[18] and acryloyl chloride, with triethylamine as the base and DMAP (4-Dimethylaminopyridine) as the catalyst. The synthesis of 3-vinyl oxadiazole **10** (Scheme 2) started with 3-acetylbenzonitrile, which was converted to tetrazole **7** by refluxing with NaN_3 and $ZnBr_2$ in water.[19] The crude tetrazole **7** was then reacted with 4-*tert*-butylbenzoyl chloride in pyridine at reflux. The reaction is quite clean, affording a crude product that was recrystalized in ethanol to give oxadiazole **8**. Reduction of **8** with $NaBH_4$ gave oxadiazole **9**, which was dehydrated to the final vinyl oxadiazole monomer **10**. Although this sequence proceeded with acceptable yields (63% over four steps) with only

(10) (a) Gong, X.; Robinson, M. R.; Ostrowski, J. C.; Moses, D.; Bazan, G. C.; Heeger, A. J. *Adv. Mater.* **2002**, *14*, 581. (b) Jiang, C.; Yang, W.; Peng, J.; Xiao, S.; Cao, Y. *Adv. Mater.* **2004**, *16*, 537.
(11) (a) Bulovic, V.; Khalfin, V. B.; Gu, G.; Burrows, P. E.; Garbuzov, D. Z.; Forrest, S. R. *Phys. Rev. B* **1998**, *58*, 3730. (b) Forrest, S. R.; Bradley, D. D. C.; Thompson, M. E. *Adv. Mater.* **2003**, *15*, 1043.
(12) Gong, X.; Wang, S.; Moses, D.; Bazan, G. C.; Heeger, A. J. *Adv. Mater.* **2005**, *17*, 2053.
(13) For reviews see: (a) Matyjaszewski, K. *Chem.—Eur. J.* **1999**, *5*, 3095−3102. (b) Hawker, C. J.; Bosman, A. W.; Harth, E. *Chem. Rev.* **2001**, *101*, 3661−88. (c) Kamigaito, M.; Ando, T.; Sawamoto, M. *Chem. Rec.* **2004**, *4*, 159−175. (d) Moad, G.; Rizzardo, E.; Thang, S. H. *Aust. J. Chem.* **2005**, *58*, 379−410.
(14) Benoit, D.; Chaplinski, V.; Braslau, R.; Hawker, C. J. *J. Am. Chem. Soc.* **1999**, *121*, 3904.
(15) Boiteau, L.; Moroni, M.; Hilberer, A.; Werts, M.; De Boer, B.; Hadziioannou, G. *Macromolecules* **2002**, *35*, 1543.
(16) (a) Behl, M.; Hattemer, E.; Brehmer, M.; Zentel, R. *Macromol. Chem. Phys.* **2002**, *203*, 503. (b) Behl, M.; Zentel, R. *Macromol. Chem. Phys.* **2004**, *205*, 1633.
(17) Fichet, G.; Corcoran, N.; Ho, P. K. H.; Arias, A. C.; Mackenzie, J. D.; Huck, W. T. S.; Friend, R. H. *Adv. Mater.* **2004**, *16*, 1908.
(18) Furuta, P.; Fréchet, J. M. J. *J. Am. Chem. Soc.* **2003**, *125*, 13173.
(19) Demko, Z. P.; Sharpless, K. B. *J. Org. Chem.* **2001**, *66*, 7945.

Scheme 1[a]

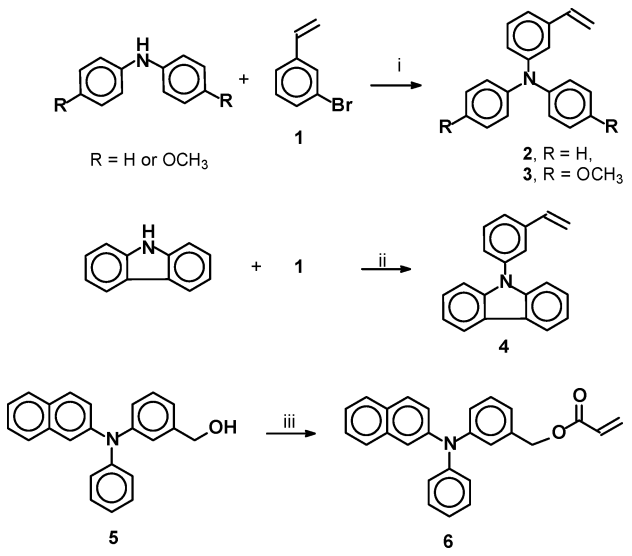

[a] Conditions: (i) NaO-*t*-Bu, $Pd_2(dba)_3$, P(*t*-Bu)$_3$, toluene, 0 °C to room temperature; (ii) NaH, $Pd_2(dba)_3$, P(*t*-Bu)$_3$, toluene, 80 °C; (iii) acryloyl chloride, DMAP, Et_3N, CH_2Cl_2.

filtration and recrystallization, an alternative route was also explored for 4-vinyl oxadiazoles **13** and **14**, in which bromides[20] **11** and **12** were coupled with tributylvinyltin using $Pd(PPh_3)_4$ as the catalyst. Acrylate ET monomer **18** was constructed by first coupling protected tetrazole **15** with benzoyl chloride and then removing the protecting group with TBAF (Tetrabutylammonium fluoride) to afford oxadiazole **16**, which was acylated with acryloyl chloride to afford the final oxadiazole **18**. Acrylate **19** was produced in a similar manner from **15** and 4-*tert*-butylbenzoyl chloride. Diketone ligand monomers were constructed by reacting 4-chloromethylstyrene with either acetylacetone or 2,6-dimethyl-3,5-heptanedione, yielding **20** and **21**, respectively (Scheme 3), which were used later to incorporate iridium or platinum complexes into the polymers. Additionally, monomers **22**,[21] **23**,[22] **24**,[23] and **25**[15] were also synthesized according to literature procedures.

Homopolymers. The newly synthesized monomers were polymerized using alkoxyamine **26**[14] as the initiator. The polymerizations were run neat at 125 °C, except in the case of **25**, where *tert*-butylbenzene was used as a solvent at 3 M concentration because of the high melting point of **25**. The MWs of the polymers (Table 1) were determined by size exclusion chromatography (SEC) using polystyrene standards. Multi-angle laser light scattering (MALLS) analysis was also performed on a few polymers. It was found that the theoretical MWs of the polymers predicted based on the initiator-to-monomer ratio matched the light scattering results reasonably well, while the polystyrene standards underestimated the MWs of most polymers. The homopolymers prepared from vinyl triphenylamine monomers **2** (polymers **28**−**30**) and **22** (polymer **42**) as well as oxadiazole monomer **25** (polymer **47**) showed good polydispersity indexes (PDI)s, while slightly broader PDIs were observed for polymers prepared from vinyl oxadiazole monomers **10** (polymer **34**), **13** (polymers **35**−**36**), **14** (polymer **37**), and **24** (polymers **44**−**46**) and acrylate monomers **6** (polymer **33**), **18** (polymer **38**), **19** (polymer **39**), and **23** (polymer **43**). The difference in PDI for polymer **47** compared with those for polymers

Scheme 2[a]

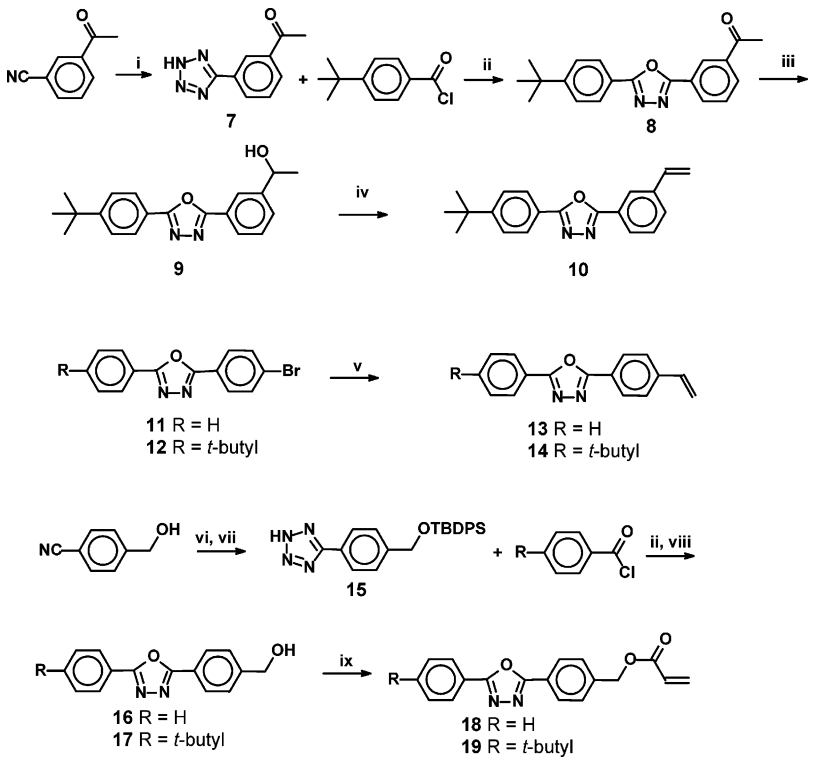

[a] Conditions: (i) NaN_3, $ZnBr_2$, water, reflux; (ii) pyridine, reflux; (iii) $NaBH_4$, EtOH, room temperature; (iv) PTSA (p-Toluenesulfonic acid), toluene, reflux; (v) $Pd(PPh_3)_4$, tributyvinyltin, toluene, 90 °C; (vi) TBDPSCl (*tert*-Butyldiphenylsilyl chloride), imidazole, DMF; (vii) NaN_3, $Et_3N{\cdot}HCl$, toluene, 100 °C; (viii) TBAF, THF; (ix) acryloyl chloride, Et_3N, DMAP, CH_2Cl_2.

Table 1. Homopolymerization of Various Monomers Initiated by Nitroxide 26[a]

polymer	monomer	reaction time (h)	conv (%)	GPC M_w[b]	GPC PDI	theoretical M_w[c]
28	**2**	18	91	18 000 (32 000[d])	1.15	29 000
29	**2**	2.0	64	10 000	1.18	16 000[e]
30	**2**	0.75	36	5 400	1.15	7 000[e]
31	**3**	18	63	11 000	1.33	19 000[e]
32	**4**	17	99	21 000	1.60	27 000
33	**6**[f]	16	92	14 000	1.89	15 000
34	**10**	15	95	30 000	1.40	33 000
35	**13**	15	93	23 000 (38 000[d])	1.47	36 000
36	**13**[f]	5.0	70	14 000	1.19	23 000[e]
37	**14**	15	89	21 000	1.61	29 000
38	**18**[f]	17	49	14 000 (23 000[d])	1.31	20 000[e]
39	**19**[f]	17	58	7 300	1.39	13 000[e]
40	**20**	5.0		15 000	1.22	12 000
41	**21**	4.0	89	16 000	1.12	19 000
42	**22**	20	67	3 200	1.11	9 000[e]
43	**23**[f]	20	86	13 000	1.44	17 000
44	**24**	0.7	37	6 100	1.29	12 000[e]
45	**24**	2.0	61	25 000	1.19	40 000[e]
46	**24**[g]	18	90	25 000	2.25	29 000
47	**25**	20	90	17 000 (32 000[d])	1.13	35 000
48	NVK[h]	1	81	40 000	2.65	33 000

[a] Polymerized neat (except **25**) with initiator **26** at 125 °C except where noted. [b] M_w based on polystyrene standards, except where noted. [c] Theoretical MW based on monomer/initiator ratio, except where noted. [d] M_w based on light scattering data. [e] Theoretical M_w based on percent conversion. [f] A total of 0.05 equiv of **27** per 1 equiv of **26**. [g] Reaction temperature = 110 °C. [h] *N*-vinylcarbazole.

Scheme 3[a]

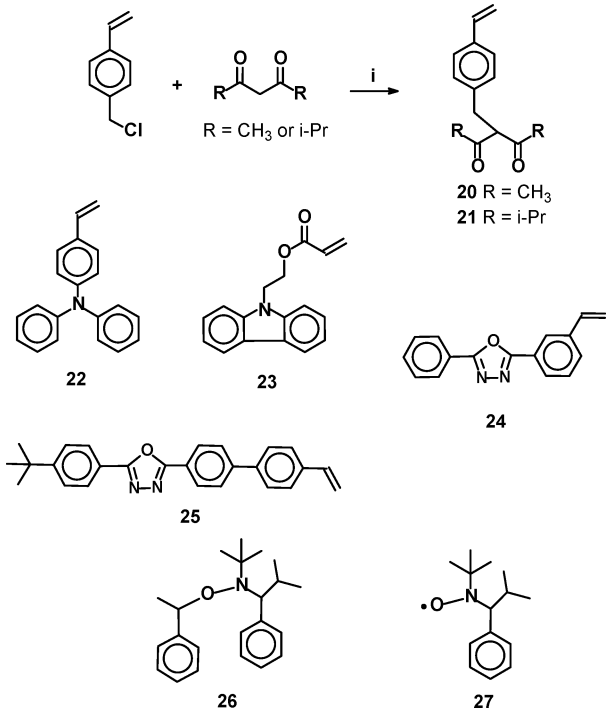

[a] Condition: (i) NaOH, NaI, DMF, 80 °C.

from other vinyl oxadiazoles (polymers **34**−**37**, **44**−**46**) is thought to be attributed to the extra phenyl ring of monomer **25** contributing to the stability of the propagating radical. Both triphenylamines **4** and **22** were tacky solids and unstable in storage, while triphenylamine **2** was a dry solid which was reasonably stable at room temperature. Given the handling problems and low conversions obtained with monomer **22** (polymer **42**), triphenylamine **2** was selected for subsequent polymerizations. As reported for acrylate monomers, 0.05 equiv of free nitroxide **27**[14] per 1 equiv of initiator **26** was used for the polymerizations of monomers **6**, **18**, **19**, and **23**. Furthermore, when nitroxide **27** was added to the polymerization of the styrenic monomer **13**, the polydispersity was also significantly improved (compare polymers **35** and **36**). The polymerization rate of the monomers was noticeably higher than that of styrene,[14] with both monomers **2** and **24** showing over 55% conversion after only 2 h (Figure 1). When compared to previously reported TEMPO initiated polymerizations,[15,16] the use of **26** as an initiator is advantageous as it involves solventless polymerizations, leading to narrower polydispersities and shorter reaction times.

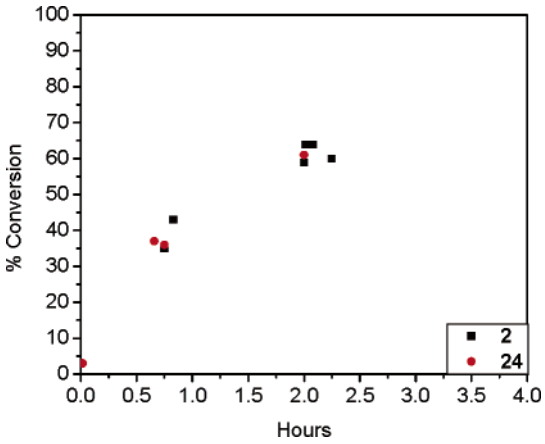

Figure 1. Conversion vs polymerization time for **2** and **24** with initiator **26**.

Table 2. Random Copolymers and Terpolymers of Various Monomers Initiated by Nitroxide 26

polymer[a,b]	monomers A/B or A/B/C	mol ratio A/B or A/B/C	M_w[c]	PDI
49	**2/14**	1/1	18 000	1.18
50	**2/14**	1/2	20 000	1.47
51	**2/14**	2/1	16 000	1.14
52	**2/19**	1/1	23 000	1.34
53	**2/25**	1/1	18 000	1.23
54	**3/24**	1/1	17 000	1.27
55	**23/24**	1/1	17 000	1.62
56	NVK/**14**[d]	1/1	13 000	1.17
57	**2/21**	8/1	8 100	1.14
58	**2/24**	1/1	19 000	1.20
59	**2/20/24**	1/1/1	13 000 (22 000[e])	1.33
60	**2/20/24**	6/1/6	17 000 (24 000[e])	1.19
61	**2/20/24**	10/1/10	14 000	1.20

[a] The average reaction time is 6 h for all polymers except for **56**, which is 15 h. [b] The isolated yield of all polymers ranges from 82% − 93%. [c] M_w based on polystyrene standards, except where noted. [d] The concentration in *tert*-butyl benzene was 3 M . [e] M_w based on light scattering data.

Copolymers. Random copolymers and terpolymers were synthesized from selected monomers and exhibited living behavior, with predictable MWs and generally low polydispersities (Table 2). While commercially available *N*-vinylcarbazole (NVK) did not exhibit living behavior with **26** as the initiator (polymer **48**), its copolymerization with **14** led to a copolymer with low polydispersity, together with a small amount of a low MW oligomer that could be removed

(20) Hou, S.; Chan, W. K. *Macromolecules* **2002**, *35*, 850.
(21) Feast, W. J.; Peace, R. J.; Sage, I. C.; Wood, E. L. *Polym. Bull.* **1999**, *42*, 167.
(22) Yatsue, T.; Miyashita, T. *J. Phys. Chem.* **1995**, *99*, 16047.
(23) Dailey, S.; Feast, W. J.; Peace, R. J.; Sage, I. C.; Till, S.; Wood, E. L. *J. Mater. Chem.* **2001**, *11*, 2238.

Table 3. Block Copolymers and Terpolymers Initiated with Macroinitiators

copolymer	initiating polymer/monomer	wt ratio polymer/monomer	M_w[a]	PDI
62	**28**/**10**	1/1	53 000	1.71[b]
63	**29**/**24**	1/2	22 000	1.23
64	**44**/**2**	1/3	16 000	1.33[b]
65	**29**/**21**	10/1	11 000	1.14
66	**65**/**24**	1/1	17 000	1.21
67	**30**/**24**	1/1	14 000	1.18

[a] M_w based on polystyrene standards. [b] Bimodal distribution.

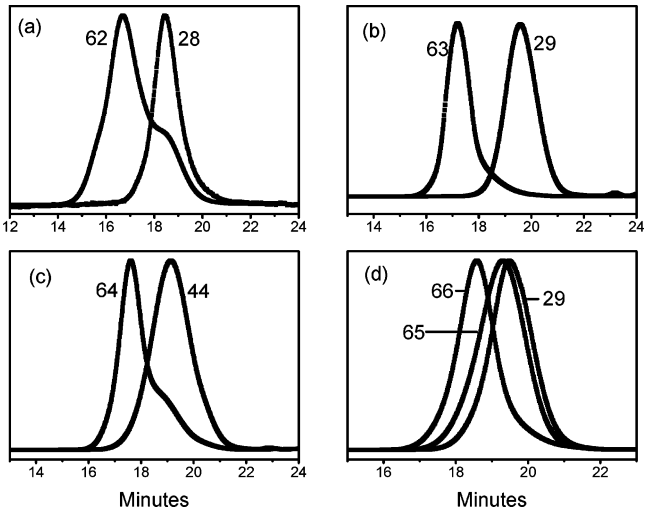

Figure 2. (a) SEC traces of triphenylamine (TPA) polymer **28** and block copolymer **62** (TPA−oxadiazole) with initiating polymer "shoulder". (b) SEC traces of TPA homopolymer **29** and copolymer **63** without significant homopolymer. (c) SEC traces of inverse block growth shows "shoulder" of initiating oxadiazole homopolymer **44** and block copolymer **64**. (d) SEC traces of initiating TPA homopolymer **29**, diblock copolymer **65**, and triblock terpolymer **66**.

by reprecipitation. The composition of these random copolymers measured by ^{1}H NMR was found to be similar to the initial ratio of the monomers, which is expected, given the high conversion of the polymerizations.

Block copolymers were also constructed, by taking advantage of the dormant nitroxide end group of homopolymers to initiate new polymerizations (Table 3). It was observed that if the initiating blocks chosen had been obtained with polymerization times that far exceeded the time required for complete conversion (4 h), varying but significant amounts of "shoulder" contamination would be observed in the size exclusion chromatograph of the resulting block copolymer, as shown in Figure 2a. The nature of the "shoulder", isolated by fractional precipitation, was determined to be the initiating block that could either be "dead" or have failed to initiate growth of the second block. When the polymerization of the initiating block was terminated before 4 h, the resulting block copolymers showed significant reduction, or even elimination, of the homopolymer "shoulder" (Figure 2b,c). This suggests that the nitroxide end groups might be subject to terminating reactions, which competed with polymerization when the rate of polymerization had significantly slowed at or near completion. However, even when the polymerization time was kept to within 4 h, the order of monomer addition was still important to grow block copolymers. When oxadiazole homopolymer **44** was used to initiate the polymerization of **2**, a small "shoulder" corresponding to the initiating polymer was present (Figure 2c). However, if the triphenylamine homopolymer was used as the macroinitiator to grow an oxdiazole block, the "shoulder" was not observed (Figure 2b). Differential scanning calorimetry analysis of copolymer **62** showed two separate glass transition temperatures at 136 and 185 °C, corresponding roughly to the expected values for the block components, triphenylamine polymer **28** (T_g 125 °C) and oxadiazole polymer **34** (T_g 182 °C), which suggested phase separation of the HT and ET domains. A triblock terpolymer consisting of HT−Ln−ET blocks was also constructed (Figure 2d). Therefore, HT polymer **29** was used to initiate the polymerization of **21**, giving diblock copolymer **65** with a relatively short block of Ln, which was then used to initiate the polymerization of **24**, affording the final triblock copolymer **66**. The SEC traces confirmed the sequential nature of the growth with retention of narrow polydispersity at each step.

Table 4. Phosphor-Functionalized Terpolymers

functionalized terpolymer	dimer	starting terpolymer	wt % complex
59-FPt	**69**	**59**	23
60-Ir	**68**	**60**	13
61-Ir	**68**	**61**	8
66-FPt	**69**	**66**	6
59-Ir	**71**	**59**	29

Phosphor Functionalization. Both random, block co- and random block terpolymers containing β-diketone groups could be functionalized with iridium and platinum complexes. Iridium dimer **68**[24] and platinum dimer **69**[25] (Scheme 4a), with moderate solubility, were coupled to the diketonate ligands in the polymers (Scheme 4b). The copolymer and 3 equiv of dimer per 1 equiv of diketone were reacted with Na_2CO_3 at 85 °C for about 5 h in the minimum amount of solvent needed to dissolve the polymers, followed by filtration to remove insoluble starting material before reprecipitation. As an alternative, the use of soluble Ir dimer **71** (Scheme 4a) allows a complementary means of purification, in which the copolymer can be conventionally precipitated after metalation to remove excess starting dimer, a process that could be useful for functionalizing polymers that are difficult to filter or have poor solubility. While an excess of dimer and concentrated conditions were found to be necessary to attain a high degree of functionalization, the metal complexes **68** and **69** recovered from filtration and **71** recovered from the filtrate could be reused. Table 4 lists the copolymers functionalized by **68**, **69**, and **71**. The degree of functionalization could be established by ^{1}H NMR, as peaks that corresponded to the diketonate ligand and benzyl protons at ∼2.8, 3.3, and 3.7 and the enol proton at ∼16.7 ppm, would resolve to a single peak (benzyl protons) at 3.48 ppm after complete metalation (Figure 3). The 4′,6′-difluorophenylpyridine ligand also contains a unique peak at ∼8.9 ppm due to the proton at the 5′ position of the phenyl ring of the ligand, which does not overlap with other aromatic protons of the polymer.

(24) Adachi, C.; Baldo, M. A.; Thompson, M. E.; Forrest, S. R. *J. Appl. Phys.* **2001**, *90*, 5048.
(25) Brooks, J.; Babayan, Y.; Lamansky, S.; Djurovich, P. I.; Tsyba, I.; Bau, R.; Thompson, M. E. *Inorg. Chem.* **2002**, *41*, 3055.

Scheme 4[a]

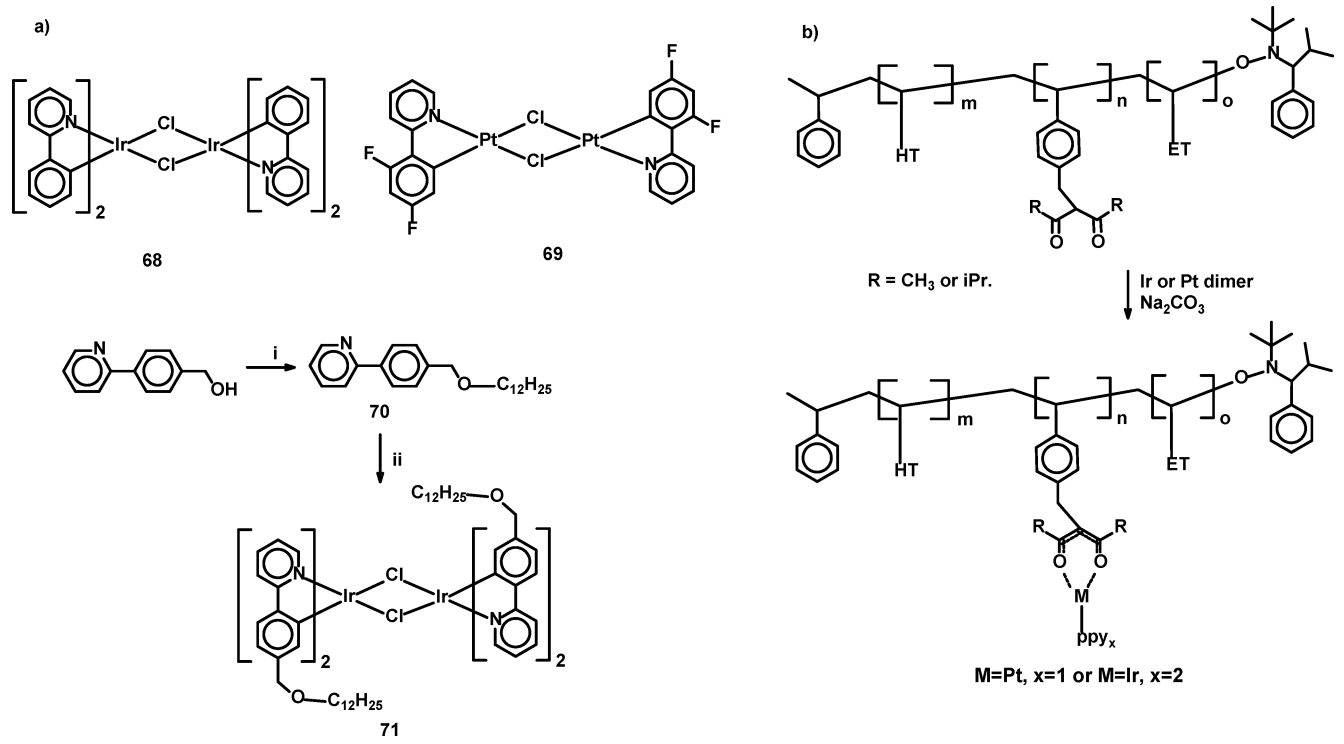

[a] (a) Structures of dimer species **68** and **69** and synthesis of the soluble dimer **71**. Conditions: (i) 1-dodecyl bromide, NaH, THF, 60 °C; (ii) $IrCl_3$, 2-ethoxyethanol, water, reflux. (b) Functionalization of diketonate polymers.

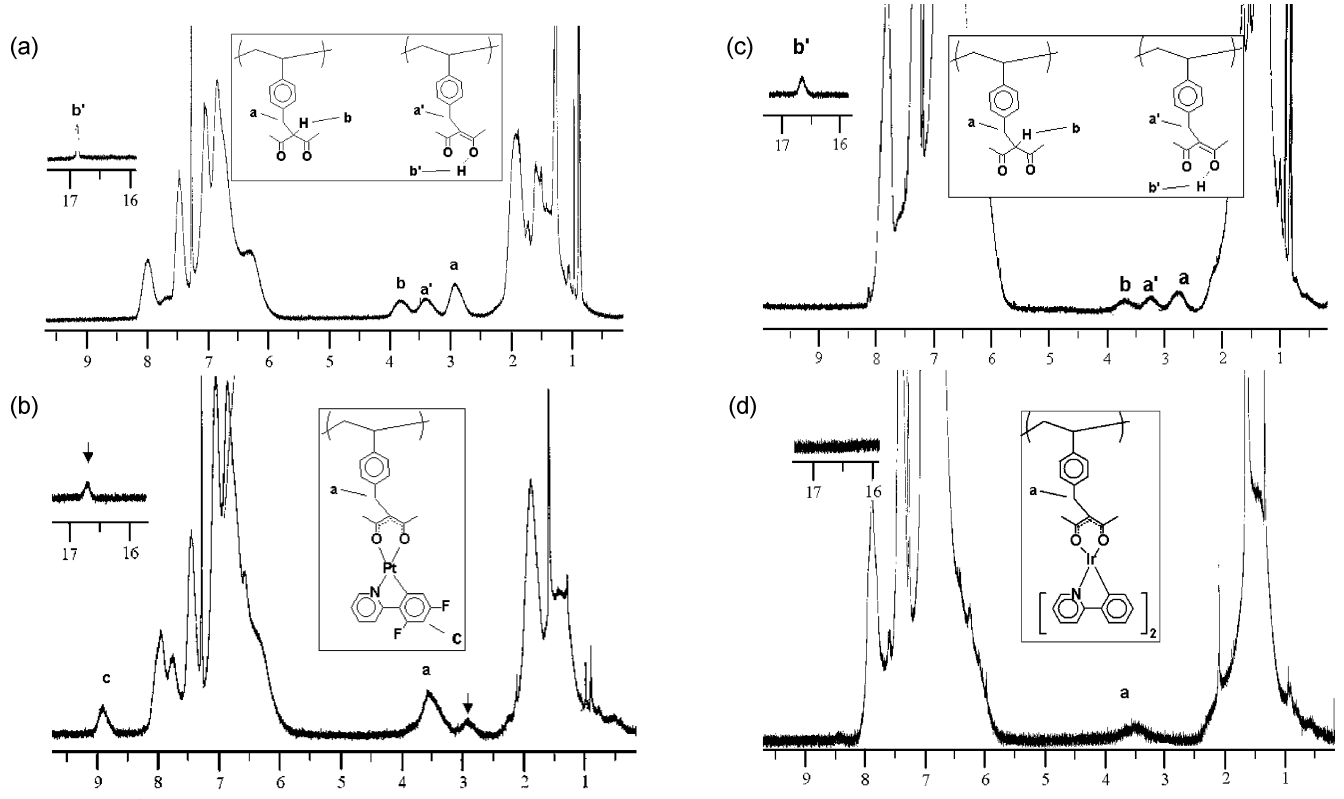

Figure 3. ^{1}H NMR: (a) Copolymer **59**, with keto form benzyl protons **a** and α-proton **b**, and enol form benzyl protons **a′** and enol proton **b′**. (b) Functionalized copolymer **59**-FPt, benzyl protons **a**, ligand phenyl proton **c**, and unreacted free acac at arrows. (c) Copolymer **60** with keto form benzyl protons **a** and α-proton **b** and enol form benzyl protons **a′** and enol proton **b′**. (d) Functionalized copolymer **60**-Ir, benzyl protons **a**, and no visible unreacted acac sites, suggesting complete functionalization.

Electrochemical Properties. Thin film cyclic voltammetry (CV) was carried out on selected copolymers to check their redox stabilities because their electrochemical behavior on thin films is more related to device performance than in solution. The results are summarized in Table 5. In thin film CV, the thickness of the diffusion layer δ is usually thinner

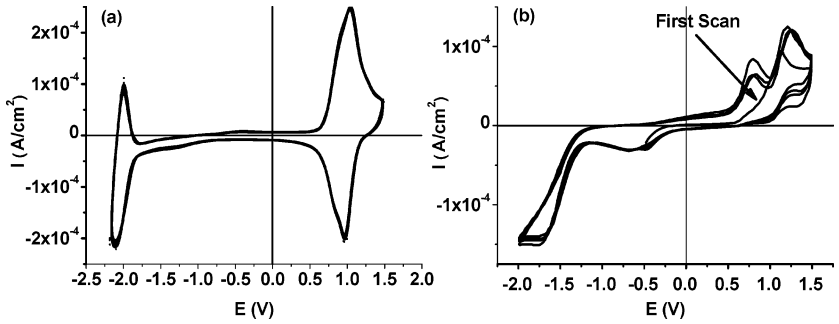

Figure 4. Cyclic voltammograms of copolymer **49** (a) as a thin film and (b) in solution.

Table 5. Redox Potentials of Bipolar Copolymers Relative to Ag^+/Ag

copolymer	$E_{1/2}^{ox}$ (V)	E_{ox}^{onset} (V)	$E_{1/2}^{red}$ (V)	E_{red}^{onset} (V)
49	1.00	0.69	−2.05	−1.85
52[a]	1.17	0.93		
53	1.15	0.78	−1.83[b]	−1.70
54[c]		0.76		−1.76
55	1.41[d]	1.28	−1.92[b]	−1.63

[a] Polymer **52** showed no reduction peak until −2.2 V. [b] Quasi-reversible reduction. [c] Irreversible oxidation and reduction. [d] Major oxidation peak.

than that of the film Φ, and charge transfer through the film occurs largely by charge hopping rather than physical motion of the redox centers, because the redox moieties are anchored to the polymer backbone.[26] Copolymers with triphenylamine as the hole transporter (copolymers **49**, **52**, and **53**) showed reversible oxidation for the thin film samples despite reports that simple triarylamines without para substitution exhibit irreversible electrochemistry.[27] We attribute the observed reversibility for the polymers to the folding of the polymer chains and the limited motion of the redox centers in the film, which could prevent the dimerization of triphenylamine radical cations. To test our hypothesis, studies involving solution CV were also carried out. As shown in Figure 4, the oxidation of copolymer **49** was no longer observed to be reversible in solution: there was no peak on the return scan corresponding to the reduction of triphenylamine radical cation. A secondary oxidation peak appeared at about 0.80 V on the following scans, as expected for the oxidation of a triphenylamine dimer. A shift of the half-wave oxidation potential was also observed for HT−ET copolymers **49**, **52**, and **53**, in the range of 0.15−0.17 V, which was likely due to the presence of different ET moieties in each of the copolymers, causing variations in the local environment surrounding the HT moieties. The reduction potential of the copolymers varied from −1.83 to −2.05 V, consistent with the structural variation on the oxadiazoles. As will be illustrated below, the redox stabilities of the copolymers can be correlated to the performance of the devices (i.e., EQE, brightness, turn-on voltage).

Photophysical Properties. To test the efficiency of energy transfer, thin films of copolymers **49**−**53** with 8 wt % of iridium(III)bis(2-(4-tolyl)pyridinato-N,$C^{2'}$)acetylacetonate [$(tpy)_2Ir(acac)$][28] were prepared and optically excited. The photoluminescence (PL) spectra of these copolymers with excitation at 325 nm are depicted in Figure 5. The PL profiles

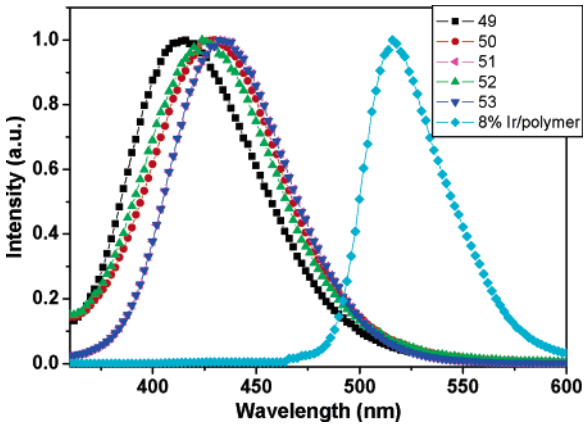

Figure 5. Normalized PL spectra of thin films of copolymers **49**−**53** and PL spectra of thin films of copolymers **49**−**53** with 8 wt % of $(tpy)_2Ir$-(acac). All the thin films had the same thickness (100 nm).

of the five copolymers tested showed a single peak exciplex emission.[29] The λ_{max} emission is between 410 and 425 nm for all of the five hosts studied. At 8 wt % $(tpy)_2Ir(acac)$, there is no polymer (exciplex) emission; only dopant emission is observed. All five hosts doped with the Ir complex follow the same behavior and only show dopant emission. This indicates that a loading of 8 wt % of $(tpy)_2Ir$-(acac) is sufficient to completely quench the host polymer emission under optical excitation. The dominant emission by $(tpy)_2Ir(acac)$ is also evidence for efficient Förster energy transfer from the copolymers to $(tpy)_2Ir(acac)$.

Devices with Copolymer Dopants. To demonstrate the suitability of HT/ET copolymers as the host matrix for phosphor dopants in OLEDs, a solution of copolymer **49** and 7 wt % of platinum(II) (2-(4′,6′-difluorophenyl)pyridinato-N,$C^{2'}$)(2,4-pentanedionato)[25] (FPt) was used to make a device with the following structure: ITO/PEDOT/dopant-copolymer/BCP/Alq_3/LiF/Al, as shown in Figure 6 (where ITO = indium tin oxide, PEDOT = poly(3,4-ethylenedioxythiophene), BCP = 2,9-dimethyl-4,7-diphenyl-1,10-phenanthroline, and Alq_3 = aluminum-tris(8-hydroxyquinolate)). In devices of this type, emission from both monomeric and aggregate states of the FPt dopant, leading to white emission, can be observed. The square planar platinum emitters were chosen here instead of the octahedral iridium

(26) Larsson, H.; Lindholm, B.; Sharp, M. *J. Electroanal. Chem.* **1992**, *336*, 263.
(27) Yano, M.; Furuichi, M.; Sato, K.; Shiomi, D.; Ichimura, A.; Abe, K.; Takui, T.; Itoh, K. *Synth. Met.* **1997**, *85*, 1665.
(28) (a) Lamansky, S.; Djurovich, P.; Murphy, D.; Abdel-Razzaq, F.; Kwong, R.; Tsyba, I.; Bortz, M.; Mui, B.; Bau, R.; Thompson, M. E. *Inorg. Chem.* **2001**, *40*, 1704. (b) Li, J.; Djurovich, P. I.; Alleyne, B. D.; Tsyba, I.; Ho, N. N.; Bau, R.; Thompson, M. E. *Polyhedron* **2004**, *23*, 419.
(29) De Lucia, F. C., Jr.; Gustafson, T. L.; Wang, D.; Epstein, A. J. *Phys. Rev. B* **2002**, *65*, 235204.

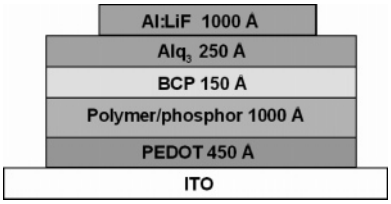

Figure 6. OLED construction: ITO/(PEDOT/PSS)/polymer-phosphor/BCP/Alq_3/LiF/Al. Both the PEDOT and polymer-phosphor layers are solution processing steps, while the BCP, Alq_3, and LiF/Al cathode layers are vacuum-deposited. The PEDOT layer acts to both planarize the substrate and efficiently inject holes into the emissive layer. The BCP/Alq_3 combination acts to efficiently block holes and inject electrons into the emissive polymer layer.

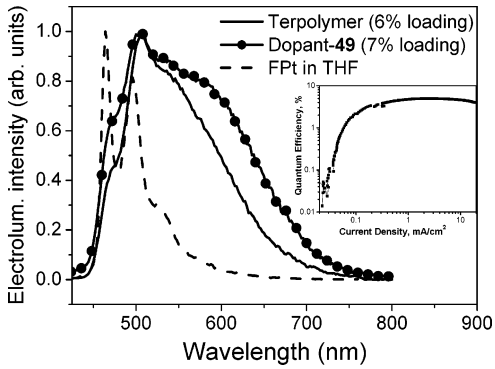

Figure 7. Emission spectrum of the FPt-doped copolymer **49** (dopant-**49**)-based OLED is compared to the spectra of the covalently anchored terpolymer one at a comparable doping level.[7f] A plot of the quantum efficiency vs current density for the dopant-**49**-based device is shown in the inset.

emitters because the platinum emitters are much more susceptible to aggregate formation.[30] Moreover, the aggregates' emission is markedly different from that of the monomer, making the detection of the two materials straightforward. Thus, the FPt emitter allows us to examine its degree of aggregation in the doped copolymer and to directly compare it to a very similar device, in which FPt was covalently anchored onto the main chain of a random HT/sty-acac/ET terpolymer.[7f] In the covalently anchored system, the FPt dopants cannot form a separate phase, because they are bound to the polymer chain. Thus, any difference between the FPt-doped copolymer **49** (dopant-**49**) device and the covalently anchored terpolymer one is likely due to dopant aggregation. The electroluminescence (EL) spectrum of the dopant-**49** device was similar to that of both terpolymer[7f] and evaporative small molecule[30] devices previously reported, showing both monomer and aggregate emissive states of FPt. The difference in excimer emission (broad shoulder, centered at roughly 600 nm) of the devices based on dopant-**49** and the covalently anchored terpolymer is consistent with the slightly higher doping level for the dopant-**49** device (7%), compared to the covalently anchored terpolymer system (6%), and is not a sign of enhanced aggregation in the dopant-**49** device (Figure 7). The maximum EQE for the dopant-**49**-based device rises sharply above a drive current of 0.02 mA/cm^2 to a stable value of 4.9%. This device efficiency compares favorably with the value of 4.6% reported for the covalently anchored system, with a similar platinum loading level.

Table 6. Properties of OLEDs Prepared from Various Polymers

polymer	turn-on voltage @ 1 Cd/m^2 [V]	maximum brightness [Cd/m^2]	maximum EQE [%]
49	8.2	8000	8.6
50	8.4	5500	9.5
51	7.5	7500	10.5
52	9.9	3500	4.0
53	10.1	3450	4.4
54	12.0	2500	3.5
55	12.4	1600	3.7
56	12.5	200	2.5
29	13.2	6	1.2

To compare different polymer hosts, solutions of homopolymer **29** and copolymers **49**−**56** with 8 wt % of $(tpy)_2Ir(acac)$ were used to fabricate OLEDs. The results are summarized in Table 6. There are several factors that can influence the performance of copolymer devices. Two of these, that is, the relative ease of charge injection and the redox stability, can be estimated by CV. Copolymers bearing triphenylamine HT (copolymers **49**−**53**) showed much better performance than copolymers with carbazole HT (copolymers **55** and **56**). We attribute the difference in performance to the higher oxidation potential of carbazole (1.28 V) relative to triphenylamine (0.69−0.93 V), which makes the hole injection more difficult for the carbazole-containing polymer.[31] Copolymers with oxadiazole **14** as ET and triphenylamine **2** as HT (copolymers **49**−**51**) showed the highest efficiencies and brightness among all the copolymers. These copolymers also showed higher redox stability than other copolymers in thin films. Devices fabricated with copolymers of different backbones illustrate the fact that copolymer with a styrenic backbone (copolymer **50**) performed better than that with an acrylic backbone (copolymer **52**). A similar finding in which the poor performance of the acrylic backbone was attributed to the high polarity and low stability of the ester functionality has been reported.[32] We also found that adding a *tert*-butyl group to the para position of the oxadiazole had a minimal effect on device performance. Last, the device performance did not appear to be affected by either the MW or the polydispersity of the copolymer used.

The ratio of ET to HT also affected the device performances. Though our devices have evaporated layers of Alq_3/BCP that slightly favor electron injection, homopolymers with unipolar HT transporter abilities still gave relatively poor device performance (polymer **29**). Device performance was greatly improved by adding ET groups to the polymer (copolymers **49**−**53**). Increasing the HT to ET ratio from 1:2 to 2:1 (copolymers **49**−**51**) lowered the turn-on voltage by about 1 V, while the EQE was increased from 8.6 to 10.5%. Copolymer **51** showed a peak EQE of 10.5%, which is the highest measured for all of the polymers tested in this study. Further tuning of the ratio of the ET to HT may well result in additional improvements in the performance of these devices.

(30) D'Andrade, B. W.; Brooks, J.; Adamovich, V.; Thompson, M. E.; Forrest, S. R. *Adv. Mater.* **2002**, *14*, 1032.

(31) Brunner, K.; van Dijken, A.; Börner, H.; Bastiaansen, J. J. A. M.; Kiggen, N. M. M.; Langeveld, B. M. W. *J. Am. Chem. Soc.* **2004**, *126*, 6035.

(32) Bellmann, E.; Shaheen, S. E.; Thayumanavan, S.; Barlow, S.; Grubbs, R. H.; Marder, S. R.; Kippelen, B.; Peyghambarian, N. *Chem. Mater.* **1998**, *10*, 1668.

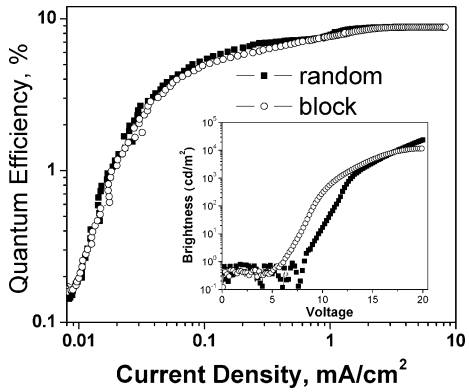

Figure 8. EQE vs current density for OLEDs with random copolymer **58** and block copolymer **67** doped with 8 wt % of $(tpy)_2Ir(acac)$ is shown. The brightness of these devices as a function of applied voltage is shown in the inset.

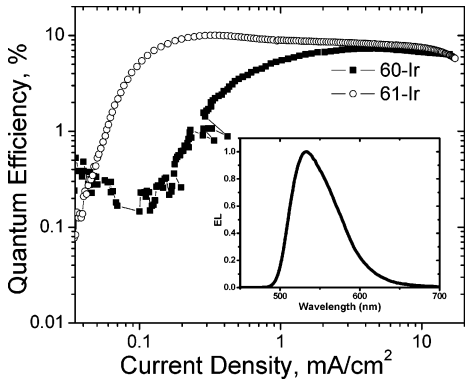

Figure 9. EQE vs current density and EL spectra (inset) for OLEDs prepared with functionalized terpolymers **60**-Ir and **61**-Ir.

We have also prepared devices with 8% $(tpy)_2Ir(acac)$ dopant in block copolymer **67** to compare with the similar random copolymer **58** (Figure 8). The devices using the block copolymer were made under exactly the same conditions as those prepared from the random copolymer; no annealing was performed to attempt control of phase segregation within the block copolymer. It is interesting to note that although the block copolymer devices had almost the same EQE as devices prepared with the random copolymer, the turn on voltage was lowered to 5.2 versus 8.2 V for the random copolymer devices. This is probably because the block copolymer has larger continuous regions of HT and ET materials than is the case for the random copolymer, which leads to greater carrier conduction and easier charge injection. Both of these factors are expected to lower the turn-on voltage. Further studies of the effect of morphology control on device performance are underway.

Devices with Functionalized Terpolymers. Functionalized terpolymers (**60**-Ir, **61**-Ir) were used to fabricate devices as shown in Figure 6, using the phosphor functionalized terpolymers for the emitting layer in place of polymer/phosphor mixtures. The emissive center in these devices is very similar to $(ppy)_2Ir(acac)$. The EQE values for **60**-Ir- and **61**-Ir-based devices are shown in Figure 9. The higher device EQE was observed with the lower doping level. The device based on **60**-Ir has a calculated iridium complex concentration of 13% and gives a peak EQE of 7.3%, while the device based on **61**-Ir, with 8% of iridium complex concentration, has the higher peak EQE of 10.0%. This suggests that the optimum concentration of the iridium complex in this polymer system is exceeded in **60**-Ir, and efficiency is lost as a result of self-quenching. This result is not surprising, because the optimal doping level for a given dopant depends strongly on the matrix. The same dopant in a triazole host shows the highest EQE at a doping level of 12%.[24] The EL spectra of the devices made from **60**-Ir and **61**-Ir (inset of Figure 9) show a sharp peak with the maximum at 512 nm, which is comparable to reported devices made with vacuum-deposited $(ppy)_2Ir(acac)$.[24] The emission spectra did not change with changing driving voltages for all devices made.

Experimental Section

General Methods. All reactions were run under N_2 unless otherwise noted. Solvents were dried as follows: tetrahydrofuran (THF) and toluene were dried over sodium. Dichloromethane, acetonitrile, pyridine, and triethylamine were distilled from calcium hydride. Chromatography was carried out with Merck silica gel for flash columns, 230−400 mesh. Unless otherwise specified, extracts were dried over Na_2SO_4 and solvents were removed with a rotary evaporator at aspirator pressure. IR spectra (KBr) were recorded on a Mattson Genesis II FTIR. NMR spectra were recorded on Bruker DRX-500 or AVX 400 instruments with tetramethylsilane or solvent carbon signals as the standards. ^1H NMR integration for polymers was normalized to benzyl (diketone) protons = 2. Elemental analyses were performed by MHW laboratories. Mass spectrometry (HRMS) using fast atom bombardment was done with a Micromass ZAB2-EZ double focusing mass spectrometer (BE geometry). Analytical SEC in THF was performed at 35 °C at a nominal flow rate of 1.0 mL/min on a chromatography line calibrated with linear poly(styrene) standards (162−2 100 000 Da) and fitted with three columns having pore sizes of 10^5, 10^3, and 500 Å, respectively. The SEC system consists of a Waters 510 pump, a Waters 717 auto sampler, a Waters 486 UV−vis detector, a Wyatt DAWN-EOS MALLS detector, and a Wyatt Optilab differential refractive index detector. Light scattering data were analyzed using Astra software from Wyatt, and SEC data using the UV−vis and differential refractive index detectors were analyzed using Millennium software from Waters. Emission spectra (PL and EL) were recorded on a PTI QuantaMaster model C-60SE spectrofluorimeter equipped with a 928 PMT detector. Film thicknesses were determined with a Rudolph Technologies ellipsometer by spin casting films onto silicon wafers.

Cyclic Voltammetry. CV was conducted using a Solatron 1285 potenstiostat. Measurements were performed using a three electrode airtight cell under nitrogen. A 2 mm diameter platinum wire was used as both the counter and the working electrodes. A Ag/AgCl electrode was used as a reference electrode. Solution CV was carried out in a mixed solvent of 7:3 CH_2Cl_2/CH_3CN, and solid-state CV was done in CH_3CN. Films for solid-state CV were prepared by dipping the working electrode into a 10 mg/mL polymer solution in $CHCl_3$ and then drying it by a stream of N_2. In both cases, 0.1 M tetrabutylammonium hexafluorophosphate was used as the supporting electrolyte. Current versus voltage mea-

surements were recorded versus the Ag/AgCl reference electrode, which had been calibrated using a standard ferrocene/ferrocenium couple.

OLED Fabrication. Prior to device fabrication, ITO on glass substrates was patterned as 2 mm wide stripes with a resistivity of 20 Ω/□. The substrates were cleaned by sonication in soap solution; rinsed with deionized water; boiled in trichloroethylene, acetone, and ethanol for 3−4 min in each solvent; and dried with nitrogen. Finally, the substrates were treated with UV ozone for 10 min. A layer of PEDOT/poly(styrene sulfonate) (PSS) was spin-coated onto the substrate at 8000 rpm and baked in air at 90 °C for 45 min. The polymer (or polymer and phosphors) was dissolved in chloroform at a concentration of 15 mg/mL. The resulting solutions were filtered (2 μm poly(vinylidene difluoride) filter) prior to use. The solutions were spin cast at 2000 rpm for 40 s. The film thickness was determined to be in the range of 1000−1200 Å by ellipsometry. A 150 Å thick layer of BCP and a 250 Å layer of Alq_3 were deposited sequentially by thermal evaporation from resistively heated tantalum boats onto the polymer-coated substrate at a rate of 2.0 Å/s. The base pressure at room temperature was (3−4) $\times$ 10^{-6} Torr. After organic film deposition, the chamber was vented and a shadow mask with a 2 mm wide stripe was put onto the substrate perpendicular to the ITO stripes. A cathode consisting of 10 Å LiF followed by 1000 Å of aluminum was deposited at a rate of 0.3−0.4 Å/s for LiF and 3−4 Å/s for aluminum. OLEDs were formed at the 2 $\times$ 2 mm squares where the ITO (anode) and Al (cathode) stripes intersected.

OLED Measurements. The devices were tested in air within 2 h of fabrication. Device current−voltage and light intensity characteristics were measured using the LabVIEW program by National Instruments with a Keithley 2400 sourcemeter/2000 multimeter coupled to a Newport 1835-C optical meter, equipped with a UV-818 Si photodiode. Only light emitting from the front face of the OLED was collected and used in subsequent efficiency calculations. EL spectra were recorded on a PTI QuantaMaster model C-60SE spectrofluorimeter.

Conclusions

Novel ET, HT, and β-diketone ligand monomers were synthesized and utilized to prepare random and block co- and terpolymers, via living radical polymerization using an alkoxyamine initiator. This system affords excellent control over the polymerization leading to materials with predictable MWs and compositions, as well as narrow polydispersities. The materials could be used successfully as a matrix doped with phosphor complexes or directly functionalized with phosphor complexes, giving both white light and efficient solution-processed OLEDs. This strategy enables facile device tuning, as both the type and the ratio of HT to ET moieties can be adjusted to maximize charge mobility and device efficiency. Devices emitting white light with maximum EQE of 4.9% and devices having green emission with maximum EQE of 10.5% have been demonstrated.

Acknowledgment. Financial support of this research (at LBNL and UCB) by the U.S. Department of Energy, Basic Energy Sciences, under Contract No. DE-AC03-76SF00098, and (at USC) by Universal Display Corporation is acknowledged with thanks.

Supporting Information Available: Synthesis and characterization of monomers and polymers and EQE graph and EL spectra of polymers **49**−**53**. This material is available free of charge via the Internet at http://pubs.acs.org.

CM051922+